Available online at www.sciencedirect.com

ScienceDirect

Photonics and Nanostructures – Fundamentals and Applications 16 (2015) 34–42

PHOTONICS AND NANOSTRUCTURES Fundamentals and Applications

www.elsevier.com/locate/photonics

Improving the efficiency of dye sensitized solar cells by TiO_2-graphene nanocomposite photoanode

Umer Mehmood [a], Shakeel Ahmed [b], Ibnelwaleed A. Hussein [a,c,*], Khalil Harrabi [d]

[a] *Department of Chemical Engineering, King Fahd University of Petroleum & Minerals, P. O. Box 5050, Dhahran 31261, Kingdom of Saudi Arabia*
[b] *Center for Refining & Petrochemicals, King Fahd University of Petroleum & Minerals, Dhahran 31261, Kingdom of Saudi Arabia*
[c] *Gas Processing Center, College of Engineering, Qatar University, P. O. Box 2713, Doha, Qatar*
[d] *Department of Physics, KFUPM, P. O. Box 5050, Dhahran 31261, Kingdom of Saudi Arabia*

Received 21 May 2015; received in revised form 22 July 2015; accepted 14 August 2015
Available online 22 August 2015

Abstract

Nanocomposite photoanodes were prepared by addition of graphene (GR) micro-platelets to TiO_2 nanoparticulate paste. TiO_2/graphene based DSSCs were fabricated using Z907 photosensitizer. Transmission electron microscope was used to confirm the presence of graphene in composite films after heating at 450 °C for 30 min. UV-visible absorption spectroscopy, photocurrent–voltage characteristics and electrochemical impedance spectroscopic measurements were conducted to characterize the DSSCs. The results show that the photo conversion efficiency is highly dependent on the concentration of graphene in the photoanode. Under an optimal conditions, solar cell based on graphene/TiO_2 shows power conversion efficiency (PCE) of 4.03%, which is about 26% greater than the cell based on pristine TiO_2 electrode (3.20%). A density functional theory was used to compute the band gap of TiO_2 and graphene-TiO_2 nano clusters.

Keywords: Nanocomposite photoanodes; Dye sensitized solar cell; Graphene; Titania; Power conversion efficiency

1. Introduction

Energy is the driving force for development, economic growth, automation and modernization. Energy usage and demand are increasing globally and researchers have taken this seriously to fulfill future energy demands [1,2]. Therefore, alternative sources of energy are needed, so that mankind can survive without depending on fossil fuels. Solar energy is one of the renewable energy sources that will contribute to the security of future energy supplies [1,2]. Solar radiation from the sun is approximately 3×10^{24} J per year, which is 10 times the current energy demands [3]. Light from the sun can be harvested by dye sensitized solar cells (DSSCs). DSSCs have got attention during the last decade due to an ideal compromise between efficiency and cost-performance [4–6]. The dye is one of the key component of the DSSCs. It absorbs light and transfer electron to the conduction band of the semiconductor. So far, polypyridyl ruthenium sensitizers based solar cells have attained up to 11% conversion efficiency [7–10]. But it is still low for commercial applications.

The major cause of low efficiency of DSSCs is the recombination of injected electrons (from the dye to the conduction band of the semiconductor) with the

* Corresponding author. Tel.: +966 532 432097.
E-mail addresses: ihussein@kfupm.edu.sa, ihussein@qu.edu.qa, organicchemistry2@gmail.com (I.A. Hussein).

http://dx.doi.org/10.1016/j.photonics.2015.08.003
1569-4410/

electrolyte termed as dark current [11–13]. Photoanode of DSSCs plays an important role in the separation and transportation of electrons. Graphene [14,15] has been proposed as an additive material for TiO_2 photoanode to increase the electron mobility, owing to their outstanding electronic properties. It has an excellent mobility of charge carrier (200,000 $cm^2\ V^{-1}\ s^{-1}$) [16] and large specific surface area (2630 m^2/g) [17]. Stoller et. al. [17] introduced graphene into TiO_2 by one step hydrothermal reaction and reported a 17.7% increase in photo conversion efficiency (PCE) of DSSC. Tang et. al. [18] embedded graphene sheets in TiO_2 paste via molecular grafting and showed 1.68% efficiency, which is five times higher than that without graphene (0.32%). Sun et. al. [19] fabricated graphene/TiO_2 nanocomposites electrode through heterogeneous coagulation method and reported 4.28% efficiency, which is 59% greater than that without graphene. However the efficiency of these cells is still lower, and the fabrication method of graphing/TiO_2 nanocompostie is relatively complex. Here, we presented a fast, economic and one-step process to prepare the graphene/TiO_2 photoanode. It is expected that the incorporation of graphene in photanode may enhance the PCE of DSSCs by reducing the charge recombination.

2. Computer simulations

All the DFT calculations were executed using Amsterdam Density Functional (ADF) program (2013.01). BAND mode was used to simulate the anatase TiO_2 clusters. The tetragonal anatase crystal structure was selected with single layer (0 0 1) surface slab. Then, we created 4×1 super cell from this slab[20]. All atoms were mapped within the unit cell. We doped the 2D-graphene sheet to find/simulate a band gap of graphene-TiO_2 nanocomposite. TiO_2 and graphene doped TiO_2 models were simulated by considering hybrid Becke parameter, Lee-Yang-Parr (B1YLP) level tohether with TZ2P (triple-ζ polarization, 2 polarization functions) and DZP (Double-ζ, 1 polarization function) as basis function, respectively. In all the calculations, relativistic effects were taken into account by the zero order regular approximation (ZORA) Hamiltonian in its scalar approximation [21].

3. Experimental

3.1. Preparation of composite anodes

A suspension of ethanol and graphene(96–99%, 50–100 nm, purchased from Grafen Chemical Industries Co, Turkey) was prepared by dissolving 20 mg of graphene in 25 ml ethanol. It was then sonicated for 3 h to attain a good dispersion of graphene in ethanol. An exact quantity of dispersed graphene was mixed with known amount of anatase TiO_2 paste (T/SP 14451, Solaronix) to obtain a composite paste. Five different samples of TiO_2-graphene were prepared by varying the composition of graphenes, i.e., 0, 0.04. 0.08, 0.12, 0.16 and 0.20 wt%. The composite paste was then tape casted on FTO glass substrate (2 mm,7 Ω/seq, Solaronix). The coated glass substrate was annealed at 450 °C for 30 min. Other photoanodes were prepared following the same procedure. The thickness of each photoanode was found by using cross sectional images obtained from SEM (JEOL, 6610LV). The average thickness of each film was 20 μm.

4. Fabrication of DSSCs

A 0.5 mM solution of the dye Z907 (cis-diisothiocyanato-(2,2′-bipyridyl-4,4′-dicarboxylic acid) -(2,2′-bipyridyl-4,4′-dinonyl) ruthenium(II)) was prepared in methanol. The composite electrodes were soaked in the dye solution for 24 h. After sensitization, the samples were washed with ethanol to eliminate unanchored dye. Pt (Plasticol T, Solaronix) layer was deposited on FTO glass substrate by tape caating technique. Then, DSSCs were fabricated employing the sensitized hybrid anode, platinum deposited counter electrode (Plasticol T, Solaronix), 60 μm sealing spacer (Meltonix 1170, Solaronix) and I^-/I_{3-} redox couple electrolyte prepared in methoxypropionitrile with a 50 mM redox concentration (Iodolyte Z-50, Solaronix).

4.1. Characterization of DSSCs

The visible spectra of Z907 in methanol and adsorbed on TiO_2 films at glass substrates were recorded with JASCO-670 UV/VIS spectrophotometer. Keithley 2400 Source Meter was used to measure the $I-V$ characteristics of the DSSCs using IV-5 solar simulator (Sr #83, PV Measurement, Inc) at AM1.5G (100 m W cm^{-2}). The silicon solar cell was used as a reference for calibration. The electrochemical impedance spectroscopy (EIS) measurements were performed in the dark using a potentiostat (Bio-Logic SAS (VMP3, s/n:0373) under a −0.7 V forward bias and a 10 mV AC amplitude, and the frequency range was 10 Hz–1 MHz.

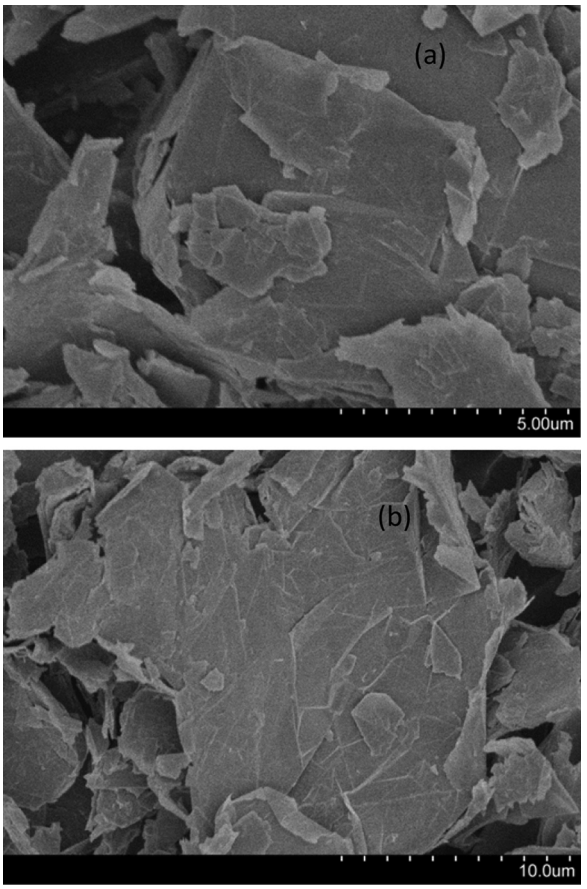

Fig. 1. SEM images of graphene sheets at different magnification; (a) 5 μm and (b) 10 μm.

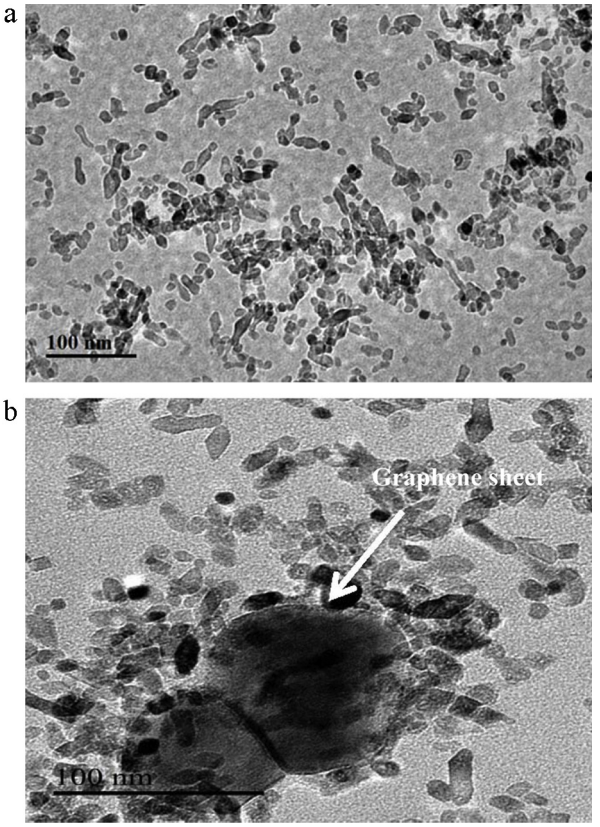

Fig. 2. TEM images of (a) TiO_2 nanoparticles and (b) TiO_2-graphene nanocomposites.

5. Results and discussion

5.1. Morphological properties of composite anode

Fig. 1 shows the SEM images of graphene microplatelets. It clearly shows the different layers of graphene. The dispersion of graphene in TiO_2 was observed by TEM (JEOL, JEM-2100F) analysis. TiO_2-graphene sample having 0.16% graphene was selected for TEM analysis, because it was difficult to obtain TEM images (of dispersed graphene in TiO_2) from low concentration samples. Fig 2(a) shows the TEM image of titania. Fig. 2(b) shows the nanocomposit of Graphen-TiO_2. It also shows that graphene nanosheets tend to congregate together to form multilayer agglomerates.

5.2. Effect of graphene on the band gap of TiO_2

The HOMOs, LUMOs and band gap energies of photosensitizers play a vital role in providing the driving force for the electron injection to conduction band of TiO_2. For efficient charge transfer, the LUMOs of dyes must be more negative than the conduction band of the semiconductor while HOMO levels must be more positive than the redox potential of electrolyte. We used a DFT technique to find the band gap of TiO_2 and graphene-TiO_2 nanocomposites. The simulated structures of TiO_2 and graphene-TiO_2 are shown in Fig. 3. While, the simulated conduction band, valence band and band gap of TiO_2 and graphene-TiO_2 are shown in Table 1. The computed results show that impregnation of graphene on TiO_2 significantly reduces the band gap of TiO_2 cluster. These results are in good agreement with the experimental values[22–24]. This is because graphene possesses lower value of the E_{CB} (∼0 eV vs.

Table 1
Simulated electronic structure properties of TiO_2 and carbon doped TiO_2.

System	E_{CB} (eV)	V_B (eV)	Simulated band gap (eV)	Experimental band gap (eV)
TiO_2	−4.10	−7.20	3.10	3.20
GR-TiO_2	−4.20	−6.95	2.75	2.90

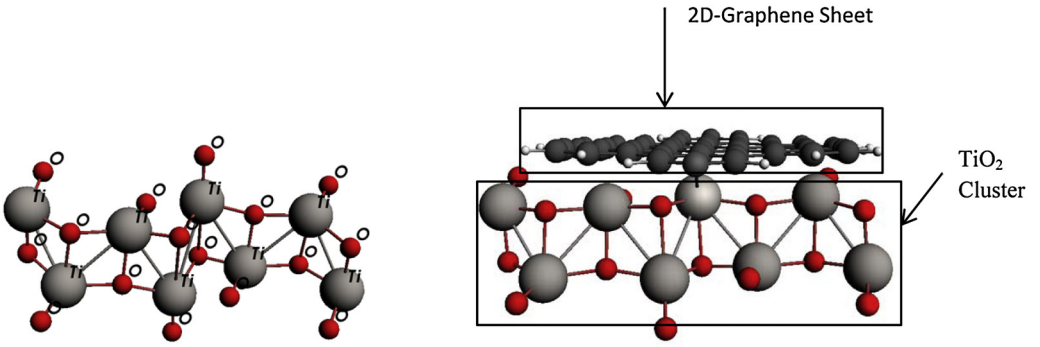

Fig. 3. Simulated structures of (a) TiO_2 and (b) carbon doped TiO_2.

NHE) [25] than that of titania (−0. 5 eV vs. NHE) [26]. The charge equilibrium between graphene and TiO_2 would cause a shift of apparent Fermi level (E_F) to more positive potential. Moreover, the downward positive shift due to graphene can cause a significant driving force to expedite the electron transport from the sensitizer to the photoanode.

6. Photophysical properties

The visible spectra of Z907 in methanol and anchored to TiO_2 and TiO_2-graphene are shown in Fig. 4(a) and (b), respectively. The two broad visible absorption bands at 525 and 380 nm in Z907 are assigned to metal-to-ligand charge-transfer (MLCT). The bands in the UV at 312 nm are assigned as intra ligand (π–π^*) charge-transfer transitions. However, the absorption shifts towards lower energy values when anchored to TiO_2 and TiO_2-graphene. This is due to the fact that on the electrode the carboxylate groups bind to the TiO_2 surface, in which Ti^{4+} acts as proton. The interaction between the carboxylate group and the surface Ti^{4+} ions may lead to increased delocalization of the π^* orbital. The energy of the π^* level is decreased by this delocalization, which explains the red shift for the absorption spectra. But the TiO_2-graphene based photoanode has a greater red shift value as compared to pure TiO_2. This is because the graphene may exhibit photosensitizing properties, thus extending photovoltaic properties into the visible spectrum [27,28].

6.1. Photovoltaic properties of DSSCs based composite anode

Hybrid graphene/TiO_2 based DSSCs were prepared with an effective area of 0.35 cm^2. The photovoltaic parameters, short-circuit current density (J_{sc}), open circuit voltage (V_{oc}), fill factor (FF), photovoltaic conversion efficiency (η), shunt resistance (R_{sh}) and series resistance (R_s) are summarized in Table 2 and the corresponding I–V curves are showed in Fig. 5. The DSSC with the highest efficiency is achieved in the case of 0.16% graphene, which is about 26% greater than the unmodified TiO_2 (3.16). This is because the incorporation of graphene increases the surface area of hybrid anode and thus more dye loading was possible. However, the little decline in V_{oc} at increasing graphene contents could be attributed to the downshift of the potential band edge of the TiO_2 conduction band. It is also observed that increase in graphene concentration from optimum level (0.16%) negatively affects the performance of DSSCs. This is because of the decrease in film transparency owing to increasing graphene contents. Another possibility of low efficiency at a high graphene concentration could be attributed to the formation of graphene agglomerates inside the TiO_2 matrix acting as trapping sites that obstruct the fast charge collection at the electrodes. The

Table 2
Photovolatic properties of DSSCs.

DSSCs	j_{sc} (mA/cm^2)	V_{oc} (mV)	FF (%)	η (%)	R_s (Ω)	R_{sh} (Ω)
Pure TiO_2	11.647	695	40	3.20	200	835
0.04%GR + TiO_2	12.142	694	41	3.36	192	899
0.08%GR + TiO_2	12.153	707	35	3.00	185	898
0.12%GR + TiO_2	16.590	714	34	3.94	132	677
0.16%GR + TiO_2	16.539	697	35	4.03	131	765
0.20%GR + TiO_2	16.201	695	32	3.69	130	588

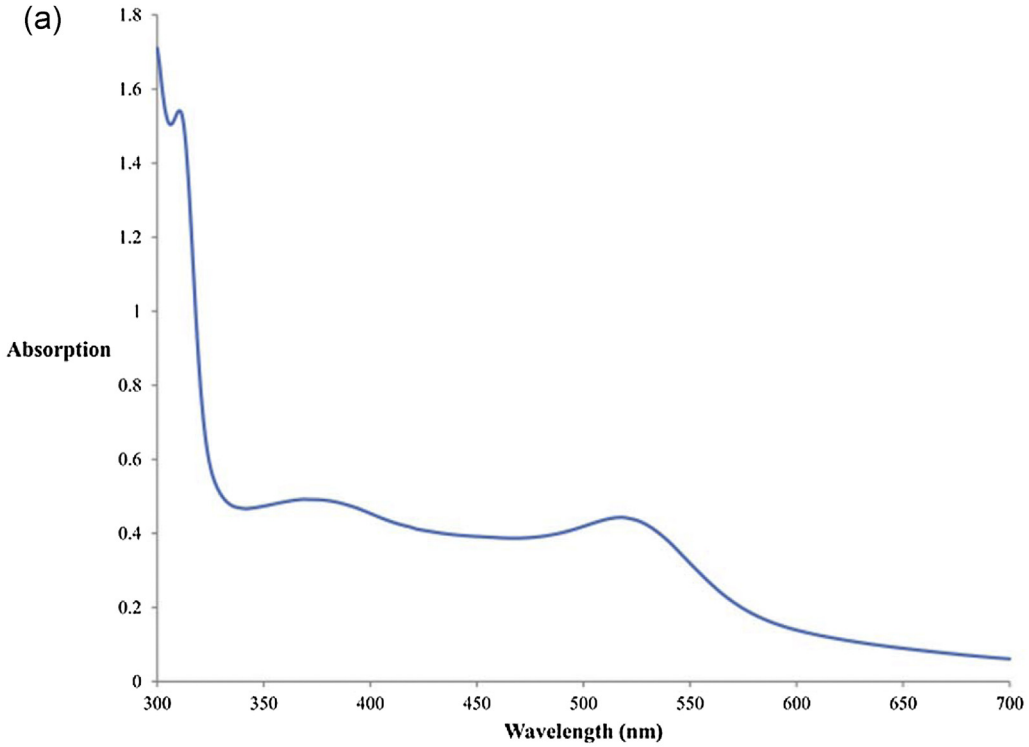

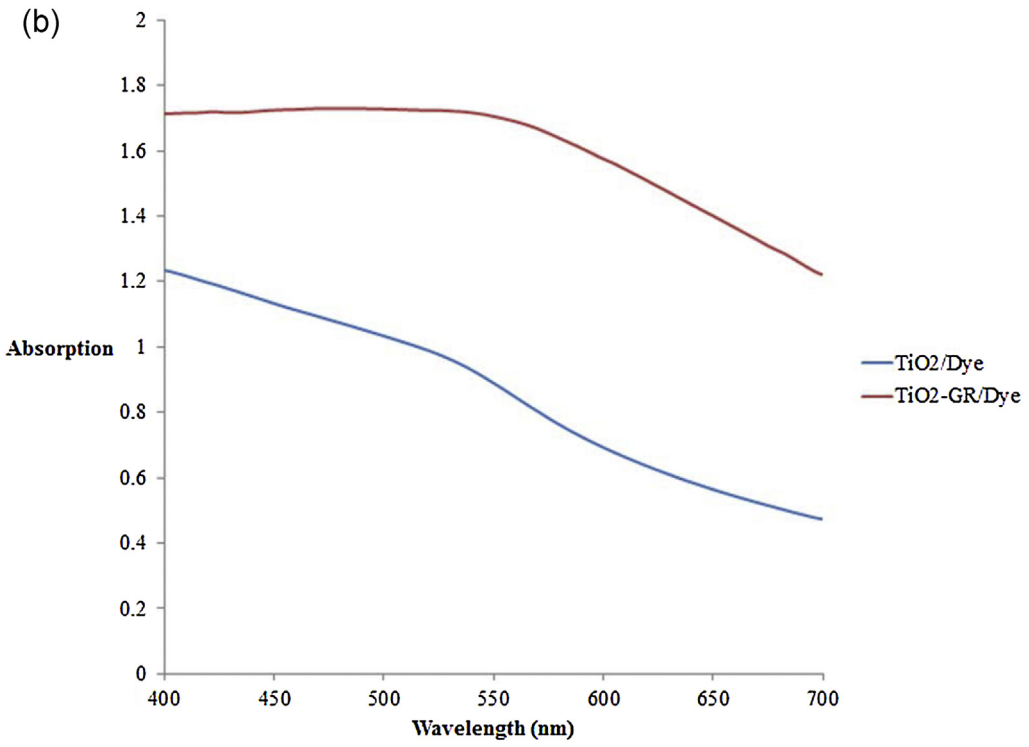

Fig. 4. (a) UV–vis spectra of Z907 in methanol and (b) UV–vis spectra of TiO_2/Z907 and 0.16%GR + TiO_2/Z907.

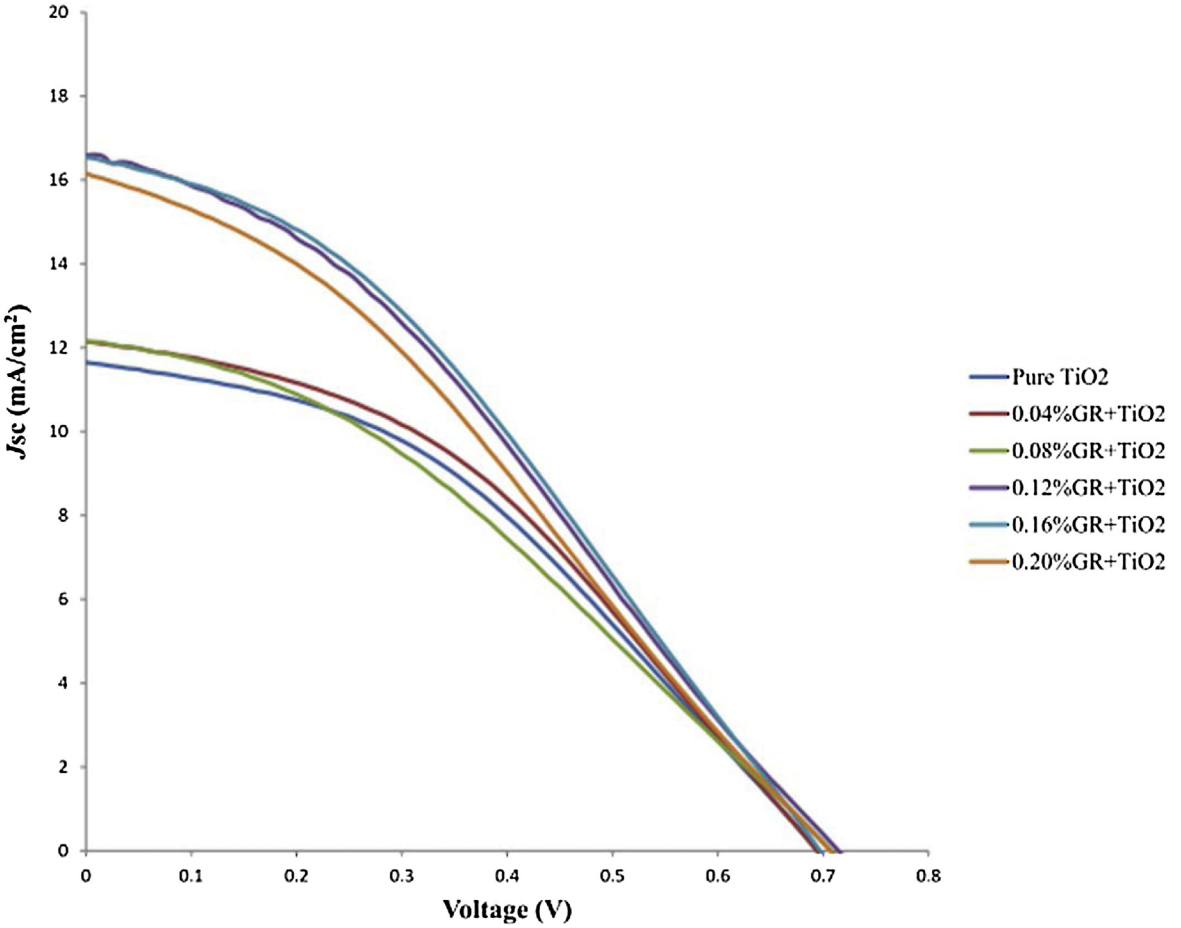

Fig. 5. Current-voltage characteristics of DSSCs fabricated using different contents of graphene.

less charge collection together with light loss owing to graphene direct absorption, strongly declines the efficiency of DSSCs at high graphene contents. As FF depends on both R_s (should be low) and R_{sh} (should be high), the FF values are low for these DSSCs (Table 2) which is supported by the measured high R_s and low R_{sh} values (Table 2). The low shunt resistance causes power losses in solar cells by providing an alternate pathway for the light-generated current, which lowers FF. R_{sh} should be of the order of 10^3 Ω for a highly efficient solar cell [29]. The high series resistance (R_s) is mainly due to large thickness of platinum counter electrode or electrolyte layer [30,31]. While low shunt resistance (R_{sh}) can be attributed to an inefficient fabrication process of DSSCs [32].

6.2. Electrochemical impedance spectroscopy

EIS analysis is performed to further explain the photovoltaic properties of DSSCs. Fig. 6 shows the Nyquist plot of DSSCs, which were assembled with TiO_2-Z907 and graphene-TiO_2-Z907. Generally, a normal impedance spectrum of DSSCs is represented by three arcs (semicircles). The first semicircle represents the charge transport resistance at counter electrode/electrolyte (R_1), second signifies the charge transport resistance at the photoanode/electrolyte interface (R_2), and the third indicates the diffusion process of redox couple in electrolyte (Z_w) [26,33]. Only second arc comes out in the Nyquist plot in the Fig. 5. It is probable that the other two arcs corresponding to R_1 and Z_w are overshadowed by larger semicircle reprinting R_2 [34,35]. The R_2 is related to the charge recombination rate, e.g., a high R_2 value shows a lower charge recombination and vise versa. The R_2 value for DSSC assembled with pure TiO_2 is smaller than that of 0.16% graphene-TiO_2, proposing charge recombination is greatly reduced owing to the incorporation of graphene. However, the graphene concentration greater than 0.16 wt% will lead to the smaller values of R_2 due

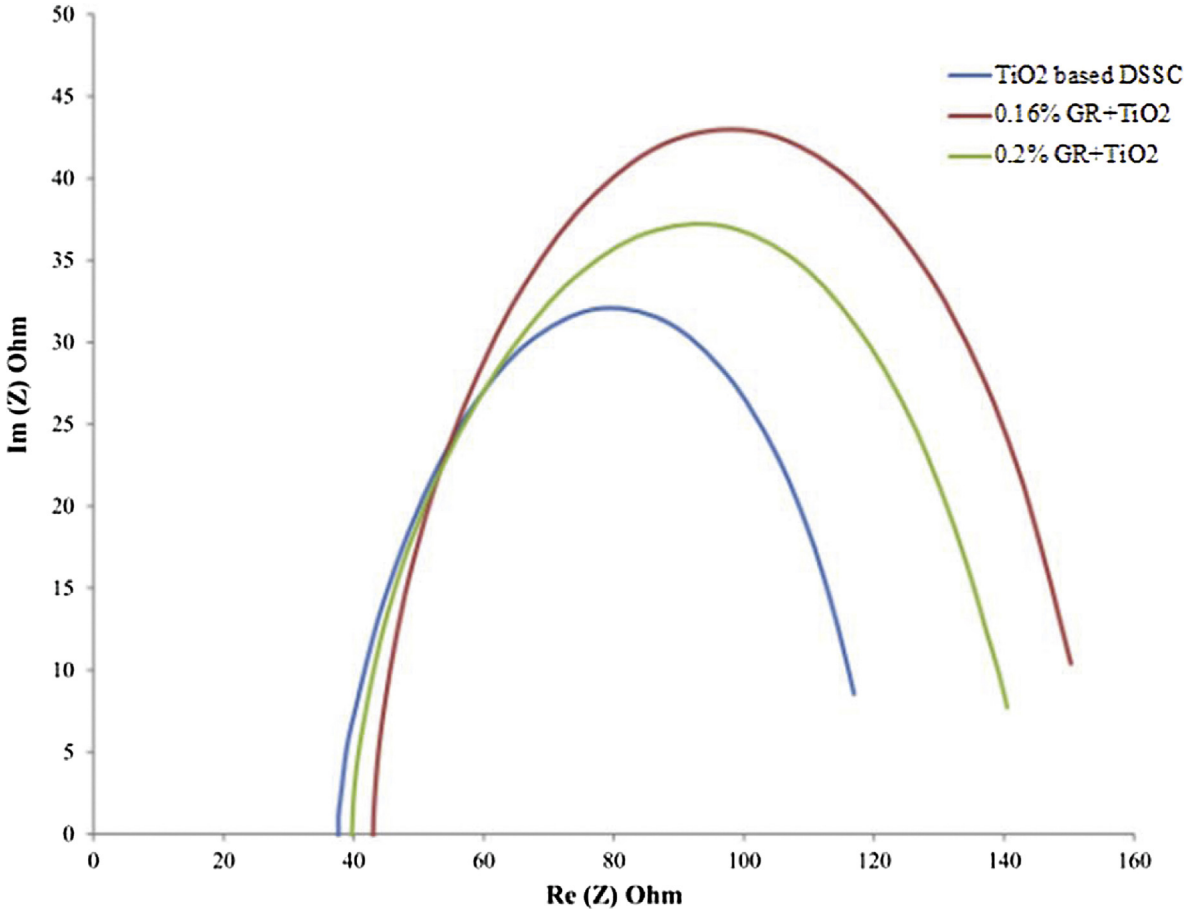

Fig. 6. EIS investigation of TiO_2 and GR + TiO_2 based DSSCs.

to a shorter electron lifetime of the order of few tens of mili seconds [36].

7. Conclusion

We established a fast and highly reproducible methodology to fabricate DSSCs by simple addition of graphene sheets into a TiO_2. The incorporation of graphene in TiO_2 is slowing the recombination of photogenerated electrons, extending the excitation wavelength and increasing the surface-adsorbed amount of dye. We established that the dispersion of small amounts of graphenes in TiO_2 can significantly improve the photo conversion efficiency of DSSCs. Optimum concentration (0.16%) of graphene in photoanode does not affect the transparency of TiO_2 layer, while significantly increases the PCE of DSSC, with a maximum value of 4.03%. Thus, we established a profligate, economical, and highly effective technique to enhance the light conversion efficiency of DSSCs.

Acknowledgment

The authors would like to acknowledge the support provided by King Abdulaziz City for Science and Technology (KACST) through the Science & Technology Unit at King Fahd University of Petroleum & Minerals (KFUPM) for funding this work through project no. 11-ENE1635-04 as part of the National Science, Technology and Innovation Plan. KFUPM is also acknowledged for supporting this research. The authors would like to acknowledge the Center of Research Excellence for Renewable Energy at KFUPM.

References

[1] K.W.J. Barnham, M. Mazzer, B. Clive, Resolving the energy crisis: nuclear or photovoltaics? Nat. Mater. 5 (2006) 161–164, http://dx.doi.org/10.1038/nmat1604.

[2] J.-L. Bredas, J.R. Durrant, Organic photovoltaics, Acc. Chem. Res. 42 (2009) 1689–1690, http://dx.doi.org/10.1021/ar900238j.

[3] K.R. Millington, Encyclopedia of Electrochemical Power Sources, Elsevier, Amsterdam, Netherlands, 2009, pp. 00317–00318, http://dx.doi.org/10.1016/B978-044452745-5.
[4] A. Hagfeldt, G. Boschloo, L. Sun, L. Kloo, H. Pettersson, Dye-sensitized solar cells, Chem. Rev. 110 (2010) 6595–6663, http://dx.doi.org/10.1021/cr900356p.
[5] N. Robertson, Optimizing dyes for dye-sensitized solar cells, Angew. Chem. Int. Ed. Engl. 45 (2006) 2338–2345, http://dx.doi.org/10.1002/anie.200503083.
[6] C. Klein, M.K. Nazeeruddin, P. Liska, D. Di Censo, N. Hirata, E. Palomares, et al., Engineering of a novel ruthenium sensitizer and its application in dye-sensitized solar cells for conversion of sunlight into electricity, Inorg. Chem. 44 (2005) 178–180, http://dx.doi.org/10.1021/ic048810p.
[7] M.K. Nazeeruddin, F. De Angelis, S. Fantacci, A. Selloni, G. Viscardi, P. Liska, et al., Combined experimental and DFT-TDDFT computational study of photoelectrochemical cell ruthenium sensitizers, J. Am. Chem. Soc. 127 (2005) 16835–16847, http://dx.doi.org/10.1021/ja052467l.
[8] F. Gao, Y. Wang, D. Shi, J. Zhang, M. Wang, X. Jing, et al., Enhance the optical absorptivity of nanocrystalline TiO_2 film with high molar extinction coefficient ruthenium sensitizers for high performance dye-sensitized solar cells, J. Am. Chem. Soc. 130 (2008) 10720–10728, http://dx.doi.org/10.1021/ja801942j.
[9] C.-Y. Chen, M. Wang, J.-Y. Li, N. Pootrakulchote, L. Alibabaei, C.-H. Ngoc-le, et al., Highly efficient light-harvesting ruthenium sensitizer for thin-film dye-sensitized solar cells, ACS Nano 3 (2009) 3103–3109, http://dx.doi.org/10.1021/nn900756s.
[10] U. Mehmood, S. Rahman, K. Harrabi, I.A. Hussein, B.V.S. Reddy, Recent advances in dye sensitized solar cells, Adv. Mater. Sci. Eng. 2014 (2014) 12, http://dx.doi.org/10.1155/2014/974782.
[11] A. Kongkanand, R.M.P. Domínguez, V. Kamat, Single wall carbon nanotube scaffolds for photoelectrochemical solar cells. Capture and transport of photogenerated electrons, Nano Lett. 7 (2007) 676–680, http://dx.doi.org/10.1021/nl0627238.
[12] K.T. Dembele, G.S. Selopal, R. Milan, C. Trudeau, D. Benetti, A. Soudi, et al., Graphene below the percolation threshold in TiO_2 for dye-sensitized solar cells, J. Mater. Chem. A 3 (2015) 2580–2588, http://dx.doi.org/10.1039/C4TA04395B.
[13] U. Mehmood, I.A. Hussein, K. Harrabi, M.B. Mekki, S. Ahmed, N. Tabet, Hybrid TiO_2–multiwall carbon nanotube (MWCNTs) photoanodes for efficient dye sensitized solar cells (DSSCs), Sol. Energy Mater. Sol. Cells 140 (2015) 174–179, http://dx.doi.org/10.1016/j.solmat.2015.04.004.
[14] J. Durantini, P.P. Boix, M. Gervaldo, G.M. Morales, L. Otero, J. Bisquert, et al., Photocurrent enhancement in dye-sensitized photovoltaic devices with titania–graphene composite electrodes, J. Electroanal. Chem. 683 (2012) 43–46, http://dx.doi.org/10.1016/j.jelechem.2012.07.032.
[15] N. Yang, J. Zhai, D. Wang, Y. Chen, L. Jiang, Two-dimensional graphene bridges enhanced photoinduced charge transport in dye-sensitized solar cells, ACS Nano 4 (2010) 887–894, http://dx.doi.org/10.1021/nn901660v.
[16] K.I. Bolotin, K.J. Sikes, Z. Jiang, M. Klima, G. Fudenberg, J. Hone, et al., Ultrahigh electron mobility in suspended graphene, Solid State Commun. 146 (35) (2008) 1–355, http://dx.doi.org/10.1016/j.ssc.2008.02.024.
[17] M.D. Stoller, S. Park, Y. Zhu, J. An, R.S. Ruoff, Graphene-based ultracapacitors, Nano Lett. 8 (2008) 3498–3502, http://dx.doi.org/10.1021/nl802558y.
[18] Y.-B. Tang, C.-S. Lee, J. Xu, Z.-T. Liu, Z.-H. Chen, Z. He, et al., Incorporation of graphenes in nanostructured TiO(2) films via molecular grafting for dye-sensitized solar cell application, ACS Nano 4 (2010) 3482–3488, http://dx.doi.org/10.1021/nn100449w.
[19] S. Sun, L. Gao, Y. Liu, Enhanced dye-sensitized solar cell using graphene-TiO[sub 2] photoanode prepared by heterogeneous coagulation, Appl. Phys. Lett. 96 (2010) 083113, http://dx.doi.org/10.1063/1.3318466.
[20] U. Mehmood, I.A. Hussein, M. Daud, S. Ahmed, K. Harrabi, Theoretical study of benzene/thiophene based photosensitizers for dye sensitized solar cells (DSSCs), Dyes Pigment. 118 (2015) 152–158, http://dx.doi.org/10.1016/j.dyepig.2015.03.003.
[21] U. Mehmood, I.A. Hussein, K. Harrabi, B.V.S. Reddy, Density functional theory study on dye-sensitized solar cells using oxadiazole-based dyes, J. Photon. Energy 5 (2015) 053097, http://dx.doi.org/10.1117/1.JPE.5.053097.
[22] Y. Zhang, S.J. Xu, Z. Sun, C. Li, C. Pan, Preparation of graphene and TiO2 layer by layer composite with highly photocatalytic efficiency, Prog. Nat. Sci. Mater. Int. 21 (2011) 467–471, http://dx.doi.org/10.1016/S1002-0071(12)60084-7.
[23] V. Stengl, S. Bakardjieva, T.M. Grygar, J. Bludská, M. Kormunda, TiO_2-graphene oxide nanocomposite as advanced photocatalytic materials, Chem. Cent. J. 7 (2013) 41, http://dx.doi.org/10.1186/1752-153X-7-41.
[24] H. Mahmood, A. Habib, M. Mujahid, M. Tanveer, S. Javed, A. Jamil, Band gap reduction of titania thin films using graphene nanosheets, Mater. Sci. Semicond. Process 24 (2014) 193–199, http://dx.doi.org/10.1016/j.mssp.2014.03.038.
[25] C.H. Tang, X.L. Dong, C. Ma, X.X. Zhang, H.C. Ma, X.F. Zhang, Constructing TiO_2/Gr with rapid electrons transfer for efficiency photocatalysis, Adv. Mater. Res. (2012) 705–708, http://www.scientific.net/AMR. 518-523.705 (accessed March 02.03.15).
[26] P. Du, L. Song, J. Xiong, N. Li, L. Wang, Z. Xi, et al., Dye-sensitized solar cells based on anatase TiO_2/multi-walled carbon nanotubes composite nanofibers photoanode, Electrochim. Acta 87 (2013) 651–656, http://dx.doi.org/10.1016/j.electacta.2012.09.096.
[27] M.-Q. Yang, Y.-J. Xu, Basic Principles for observing the photosensitizer role of graphene in the graphene-semiconductor composite photocatalyst from a case study on graphene-ZnO, J. Phys. Chem. C 117 (2013) 21724–21734, http://dx.doi.org/10.1021/jp408400c.
[28] Y. Zhang, N. Zhang, Z.-R. Tang, Y.-J. Xu, Graphene transforms wide band gap ZnS to a visible light photocatalyst. The new role of graphene as a macromolecular photosensitizer, ACS Nano 6 (2012) 9777–9789, http://dx.doi.org/10.1021/nn304154s.
[29] U. Mehmood, S. Ahmed, I.A. Hussein, K. Harrabi, Co-sensitization of TiO2-MWCNTs hybrid anode for efficient dye-sensitized solar cells, Electrochim. Acta 173 (2015) 607–612, http://dx.doi.org/10.1016/j.electacta.2015.05.132.
[30] L. Han, N. Koide, Y. Chiba, A. Islam, R. Komiya, N. Fuke, et al., Improvement of efficiency of dye-sensitized solar cells by reduction of internal resistance, Appl. Phys. Lett. 86 (2005) 213501, http://dx.doi.org/10.1063/1.1925773.
[31] P. Joshi, L. Zhang, Q. Chen, D. Galipeau, H. Fong, Q. Qiao, Electrospun carbon nanofibers as low-cost counter electrode for dye-sensitized solar cells, ACS Appl. Mater. Interfaces 2 (2010) 3572–3577, http://dx.doi.org/10.1021/am100742s.
[32] Q. Zhang, T.P. Chou, B. Russo, S.A. Jenekhe, Polydisperse aggregates of ZnO nanocrystallites: a method for energy-conversion-efficiency enhancement in dye-sensitized solar cells, Adv. Funct. Mater. 18 (2008) 1654–1660.

[33] K. Lee, C. Hu, H. Chen, K. Ho, Incorporating carbon nanotube in a low-temperature fabrication process for dye-sensitized TiO_2 solar cells, Sol. Energy Mater. Sol. Cells 92 (2008) 1628–1633, http://dx.doi.org/10.1016/j.solmat.2008.07.012.

[34] Y.-L. Xie, Z.-X. Li, Z.-G. Xu, H.-L. Zhang, Preparation of coaxial TiO_2/ZnO nanotube arrays for high-efficiency photo-energy conversion applications, Electrochem. Commun. 13 (2011) 788–791, http://dx.doi.org/10.1016/j.elecom.2011.05.003.

[35] S. Li, Y. Lin, W. Tan, J. Zhang, X. Zhou, J. Chen, et al., Preparation and performance of dye-sensitized solar cells based on ZnO-modified TiO_2 electrodes, Int. J. Miner. Metall. Mater. 17 (2010) 92–97, http://dx.doi.org/10.1007/s12613-010-0116-z.

[36] K.T. Dembele, G.S. Selopal, C. Soldano, R. Nechache, J.C. Rimada, I. Concina, et al., Hybrid carbon nanotubes–TiO_2 photoanodes for high efficiency dye-sensitized solar cells, J. Phys. Chem. C 117 (2013) 14510–14517, http://dx.doi.org/10.1021/jp403553t.